International Journal of Innovative Computing, Information and Control
Volume **12**, Number **3**, June **2016**

 ISSN 1349-4198
pp. 677–688

LANE DETECTION IN THE ABSENCE OF LANE MARKINGS FOR ROADWAY SURVEILLANCE WITH THERMAL VISION

Boon-Chin Yeo, Way-Soong Lim and Heng-Siong Lim

Faculty of Engineering and Technology
Multimedia University
Jalan Ayer Keroh Lama, Bukit Beruang, Melaka 75450, Malaysia
bcyeo@mmu.edu.my

Received October 2015; revised February 2016

Abstract. *Roadway surveillance is popular with the use of normal camera for at least two decades. Recently, thermal vision provides an alternative of machine vision for the roadway surveillance system since it demonstrates good vehicle detection accuracy, especially under night condition. Conventional lane detection method generally requires the presence of lane markings on the road. This also poses a challenge for thermal vision, in which the markings may be vague or even absent from the recorded video frames. In this paper, a Gaussian-shaped road model is proposed for lane detection in the absence of lane markings. The lane is detected based on least square method. Thus, the detected lane is considered to be the best-fit lane on the image plane. The proposed model is able to detect the center of the lane and also the width of the lane. In addition, the model also allows the determination of the shape of the lane, of whether the lane is linear or a polynomial of a certain degree.*

Keywords: Image processing, Lane detection, Roadway surveillance, Thermal vision

1. **Introduction.** Roadway surveillance has been actively researched since the last two decades by using normal camera. Many existing work is related to the accuracy improvement of vehicle detection under different lighting conditions. During the day, vehicle cast shadow was generally reported as the cause for inaccurate detection [1-3], which can be solved with shadow removal technique [4]. In the nighttime, low illumination and vehicle headlights were, however, reported for causing inaccurate detection [5-7]. Since headlights are parts of a vehicle, they were treated as the cues for vehicle detection [8], and the headlights grouping technique was later developed to improve the detection process [9].

Many vision-based vehicle detection systems require the setup of Region of Interest (ROI) to achieve a robust detection process [10,11]. Lane detection is a process to locate the lane in a traffic scene. The detected lane can be considered as the ROI that provides better localization to the detected vehicles, because all of the detected objects outside the lane can be considered as noise and therefore excluded. Lane detection is normally executed in 2 stages: lane marking detection and lane model fitting. Lane marking detection is a process of recognizing the presence of lane markings in the scene. Among the popular features for marking recognition are the marking's: color (i.e., the markings are normally brighter than the color of the road surface) [12-14], edges (i.e., sharp edges detected at the boundary of the markings) [14-16], and width (i.e., the width for every piece of detected lane markings is nearly constant) [14]. The marking detection is generally noisy and piecemeal, in which the process returns a set of coordinates that the markings are laid on. Lane model fitting is thus required to compile the collected information (in the form of coordinates) with a predefined lane model. Depending on the road geometry,

there are few choices of commonly used road models: linear model (implemented with 1st-order polynomial) [17-19], parabolic model (implemented with 2nd-order polynomial) [20], cubic model (implemented with 3rd-order polynomial) [21], splint model (implemented with piecewise polynomial) [22], and linear-parabolic model (implemented by separating the scene into far field and near field regions) [23].

Thermal vision is another choice of machine vision suitable for roadway surveillance system. Some existing work has demonstrated good vehicle detection accuracy under different lighting and weather conditions [24-29]. This is because thermal vision allows the vehicles to be apparently differentiated from the background scene. However, the quality of the lane markings under machine vision (including normal and thermal visions) varies according to the environment. The lane markings may be vague in the night time and even incomplete for an under maintained road [30]. Moreover, the common objects in the traffic scene such as trees, vehicles, shadows and street writings may also lead to the unfavorable conditions for the lane markings detection [31,32].

In this paper, a lane detection method based on road vehicle mobility is proposed to overcome the limitation. The proposed method does not require the presence of the lane markings for the lane detection. The rest of the paper is organized as follows. Section 2 and Section 3 describes the proposed road model and the lane detection method respectively. Section 4 presents the experimental results and discussions. The conclusions are drawn in Section 5.

2. **Road Modeling.**

In a traffic video recorded by a camera, every moving vehicle can be considered as moving object that presents in the scene for certain duration. These moving vehicles can be detected by the background subtraction method. The process generally requires a background model to extract the background image from the traffic video [33-37]. By comparing the background image to any frame of the traffic video, a set of coordinates will be returned to indicate the effective body region of each detected vehicle, occupying the frame. A lane on the roadway can be perceived as the path, where the vehicles normally move. For a substantial length of video processing, the coordinates collected from the background subtraction process can be assumed to be normally distributed along the center of the lane.

However, the traffic camera usually provides the images of the scene at certain perspective view. This is mainly due to the constraints of the site installation for the camera, in which the installation usually opts for large capturing area as shown in Figure 1. The lane on the xy-plane is projected onto the uv-plane that is also known as the image plane. The nearer the lanes is towards the camera, the larger the lane appears on the image plane. When the two parallel boundary lines are very far away from the camera and the distance approaches infinity, the lines converge to a vanishing point on the image plane.

Every point on the xy-plane can be mapped to a point on the image plane according to the principle of perspective projection [13,38]. To elaborate, the points $p(x, y)$, $q(x, y)$, $r(x, y)$ and $s(x, y)$ are respectively mapped to the points $p'(u, v)$, $q'(u, v)$, $r'(u, v)$ and $s'(u, v)$. Equation (1) shows the equation for the perspective mapping of the points. On the xy-plane, the width of the lane is constant at any value of x such that $|\overrightarrow{sp}| = |\overrightarrow{rq}| = \Delta y$. However, the lane on the image plane does not have a constant width such that $\left|\overrightarrow{s'p'}\right| \neq \left|\overrightarrow{r'q'}\right|$. At $x = X$, the derivative of u with respect to y proves that the lane width Δu on the image plane is linearly dependent to v. The linear relation is shown in Equation (2).

$$\frac{u}{f} = \frac{y}{x}; \quad \frac{v}{x - f} = \frac{h}{x} \tag{1}$$

$$\Delta u = \Delta y - \frac{\Delta y}{h} v \tag{2}$$

With this, a Gaussian-shaped road model is proposed as shown in Equation (3). For any value of v such that $v = V$, the model $L(u, V)$ presents a Gaussian curve. If the Gaussian curve is normalized to a Gaussian distribution function, the probability of detecting a vehicle at any point on the lane can be known. The center of the lane will have the highest probability, in which a vehicle is detected.

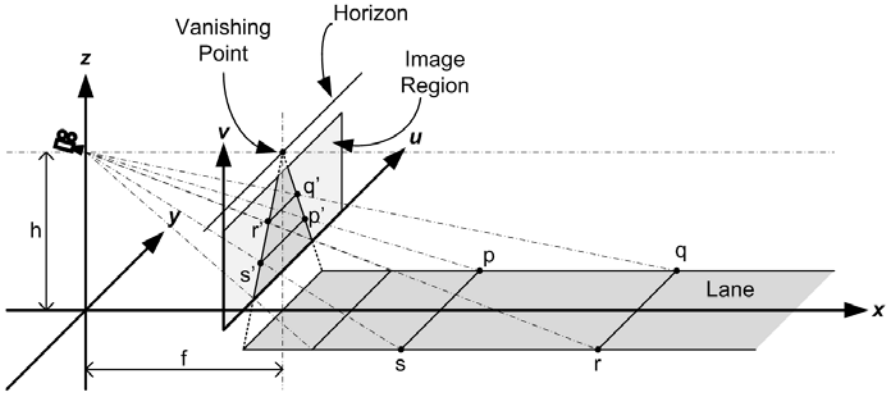

FIGURE 1. Relation between image coordinate system and the world coordinate system. The lane is laid on the xy-plane, which is projected onto the uv-plane (also known as image plane). The image region is bounded due to the limitation of the scope of camera.

The amplitude $A(v)$ is assumed to vary due to imperfect vehicle detection process in practice. Normally, the detection process is only able to detect partial body of the vehicles. The mean $\mu_u = f(v)$ is the function of a line indicating the center of the lane. Depending on the geometry of the road, the function $f(v)$ can be any polynomial function of different orders. The standard deviation σ_u can be related to the lane width. By assuming 95% of the detected points from vehicle detection process to be located within the lane, the standard deviation σ_u can be made equal to the quarter of the lane width. 5% tolerance is allocated for any incident that requires a driver to drive way from the lane. Since the lane width on the image plane is linear dependent to v, the standard deviation σ_u is therefore modeled as a linear equation, in which k_1 and k_2 are constants.

$$L(u, v) = A(v) \cdot e^{-\frac{(u-\mu_u)^2}{2\sigma_u^2}} \tag{3}$$

where

$$\mu_u = f(v) = \sum_{i=0}^{n} a_i \cdot v^i \tag{4}$$

$$\sigma_u = k_1 v + k_2 \tag{5}$$

3. **Lane Detection.** Using the developed road model in Section 2, a lane in the traffic scene can be detected in three stages: (i) vehicle detection and 2D-histogram generation, (ii) histogram fitting and normalization with Gaussian function, and (iii) lane fitting with different orders of polynomials.

In this paper, Extended Fuzzy Running Average (EFRA) background model is used for vehicle detection, since the model provides good selectivity performance for roadway surveillance under thermal vision [39,40]. EFRA has the capability of extracting the background images from a video and it is also able to extract the foreground image for

every video frame. Every detected vehicle in the scene is shown as a group of white pixels in the foreground image. Since the vehicles are normally moving on the lane, the white pixels also indicate the region of the lane. Here, we consider every white pixel on the foreground image as a coordinate on the uv-plane. And, the coordinates collected from the vehicle detection process throughout the entire recorded video are assumed to be a set of raw data. And, the raw data can be graphically represented with a 2D-histogram, showing the frequency of detected vehicles with respect to the coordinate (u, v).

Since the detected coordinates are corresponding to the vehicles on the lane, the 2D-histogram will be a surface curve, having a shape similar to the model in Equation (3). Thus, fitting the 2D-histogram to the model will result in the parameters that locate the lane in the video. For every value of v such that $v = V$, the histogram fitting process leads to a Gaussian curve $L(u, V)$ with amplitude $A(V)$, mean $\mu_u(V)$ and standard deviation $\sigma_u(V)$. Here, the traditional least square method is used in the fitting process.

The mean μ_u and the standard deviation σ_u vary according to v, as shown in Equation (4) and Equation (5) respectively. Thus, the Gaussian parameters collected from the earlier fitting process can be further fitted onto the mentioned two equations. Fitting $\sigma_u(V)$ to Equation (5) can be a simple process as the linear equation has only two parameters k_1 and k_2 to be determined. From Equation (4), the center of a lane is indicated by the mean μ_u, which can be a polynomial of any degree. The converged results provided by least square method greatly rely on the initial condition, especially for high order polynomial [41]. However, a random initial condition does not affect the converged results of a degree-1 polynomial, for instance, a random initial condition results the same coefficients a_0 and a_1 for degree-1 polynomial. This is because least square estimation for a degree-1 polynomial is actually a simple linear regression [42]. However, a random initial condition may produce different coefficients for high degree polynomial, giving an irrelevant fitted curved for the center of the lane. In this case, multiple regression can be applied in the fitting process for high degree polynomial [43]. In this method, the initial condition of the coefficients $(a_0, a_1, \ldots, a_{n-1})$, except the coefficient a_n for a degree-n polynomial, are made to be equal to the coefficients of a previously fitted degree-$(n-1)$ polynomial. Meanwhile, the coefficient a_n is initialized to zero. The fitting process will determine the value of a_n by compromising $(a_0, a_1, \ldots, a_{n-1})$. Thus, the fitted degree-n polynomial can be perceived as a curve that is fitted better (with lesser error) than the fitted degree-$(n-1)$ polynomial.

4. Experimental Results.

The three stages of the lane detection process are individually tested and discussed in the following subsections respectively.

4.1. Vehicle detection.

The traffic video in this study was recorded using a thermal camera on a sunny morning. A video length of 1 minute with frame rate of 30 frames per second was recorded. In the chronological order, the left column of Figure 2 presents some of the video frames from the video. Only one of the two lanes is used at the time, when the video was recorded. The targeted road is specifically selected due to the absence of lane markings in separating the two lanes of the road.

The middle and the right columns of Figure 2 present the background and the foreground images respectively, which were extracted with EFRA for different video frames. Generally, there are 4 vehicles approaching the camera from far. Due to the perspective view of the camera, the vehicles in the video frames look smaller at the back, but gradual increase in size as they move forward. Every white pixel in the foreground images indicate the body regions of the vehicles. Since the vehicles are normally moving on the lane, the white pixels also indicate the region of the lane. Here, we consider every white pixel on

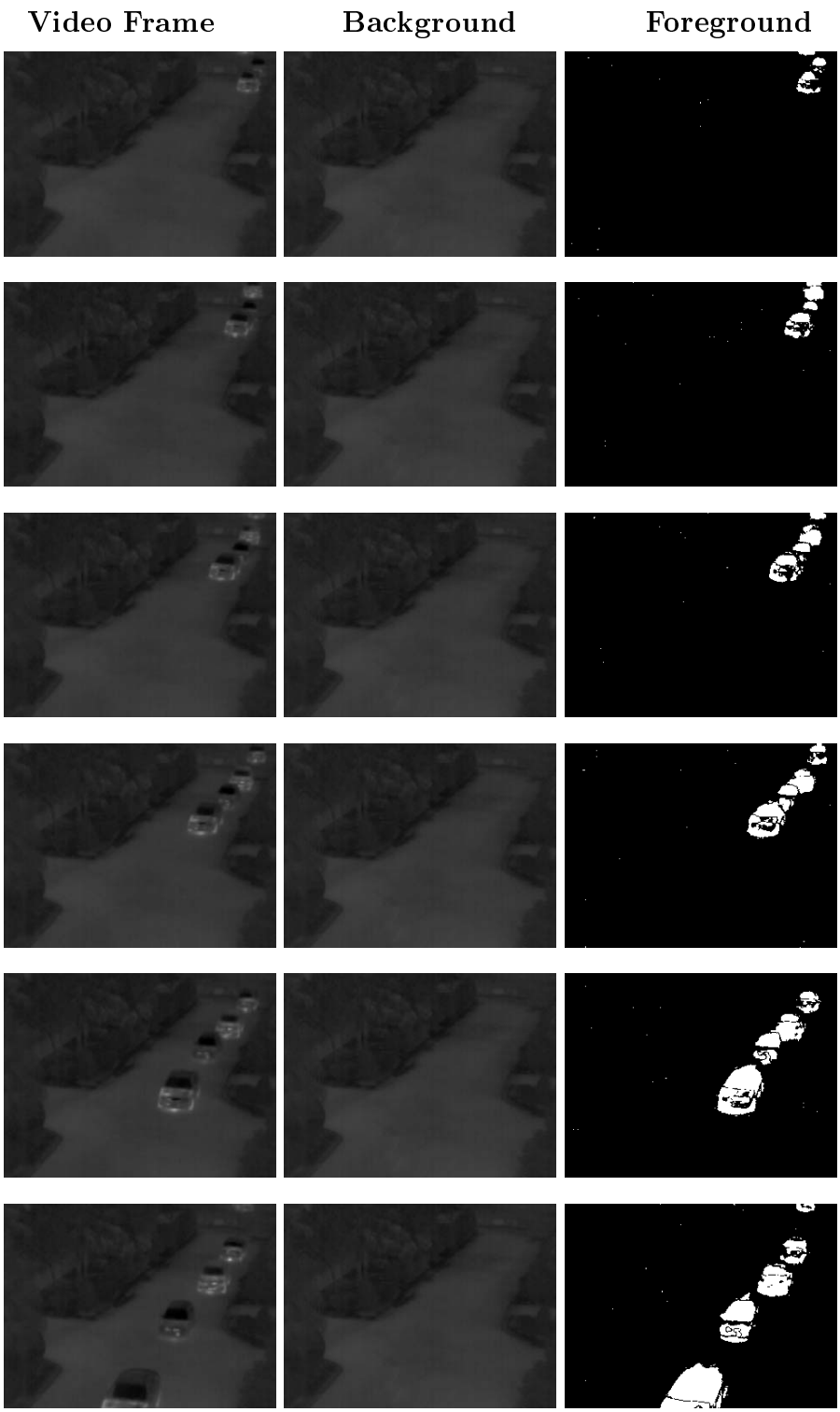

FIGURE 2. Vehicle detection with EFRA. The left column presents some example video frames. The middle column presents the background image extracted by EFRA. The right column presents the foreground image locating the vehicles in the video frames.

the foreground image as a coordinate on the uv-plane. And, the coordinates collected from the vehicle detection process throughout the entire recorded video are assumed to be a set of raw data.

A histogram can be used to graphically represent the distribution of the raw data as shown in Figure 3(a). It is observed that the highest peak for every v value is located within the road region on the image plane. Figure 3(b) presents the histograms for 3 different v values: 0, 100, and 200. These 3 histograms are Gaussian-like or bell-shaped curves with gradual decrease of the bell's width as the v value increases. Each side of the bell's width extends with a spiky horizontal lines, indicating the presence of small noise in the vehicle detection process. The height of the bell-shaped curves varies according to different v values due to the mentioned imperfect vehicle detection process. As the vehicles move closer towards the camera, more details of the vehicles can be seen. However, these details also hinder parts of the body region from being detected. Thus, the peak of the Gaussian-like curve is generally lower as v value is getting smaller.

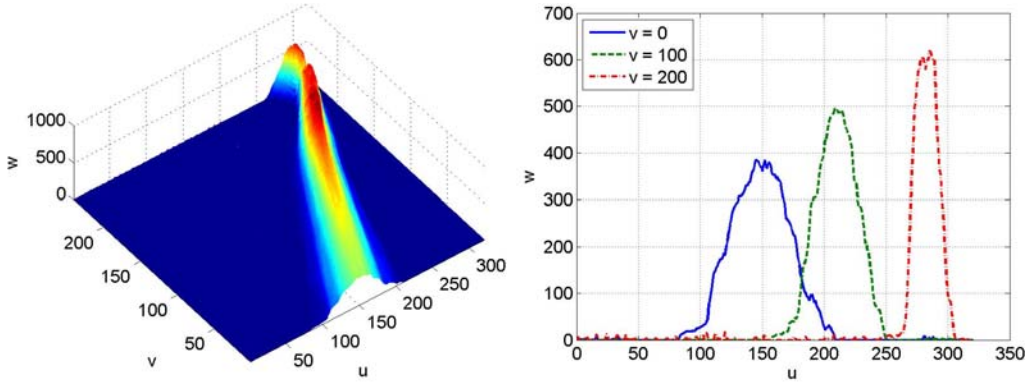

(a) (b)

FIGURE 3. Histogram of coordinates from vehicle detection process. (a) Generally, the coordinates within the road region have higher values, with the peaks at the center of the lane. (b) The opening of the bell-shaped curve becomes narrower and narrower as the v value increases.

4.2. **Histogram fitting.** The Gaussian-like histogram can be fitted onto the proposed Gaussian-shaped road model using least square method and the result is shown in Figure 4(a). The fitted model presents a smooth surface with the removal of all spiky noise. Figure 4(b) shows the fitted histograms for 3 different v values: 0, 100, and 200. The corresponding parameters of the fitted curves are shown in Table 1. Only the mean $\mu_u(v)$ (indicating the center of the lane) and the standard deviation $\sigma_u(v)$ (indicating quarter of the lane width) are essential to locate the lane on the image plane. The amplitude $A(v)$ can be excluded from lane detection. Thus, the amplitude of the model is normalized to 1 to provide better visualization of the lane. Figures 4(c) and 4(d) respectively present the normalized surface curve and the Gaussian curves for three layer cuts through the surface. The mean $\mu_u(v)$ and the standard deviation $\sigma_u(v)$ are still preserved after the normalization process.

TABLE 1. Parameters for the fitted model

v	Amplitude, $A(v)$	Mean, $\mu_u(v)$	Standard Deviation, $\sigma_u(v)$
0	386.79	148.80	23.98
100	500.26	209.93	17.02
200	666.57	282.24	9.46

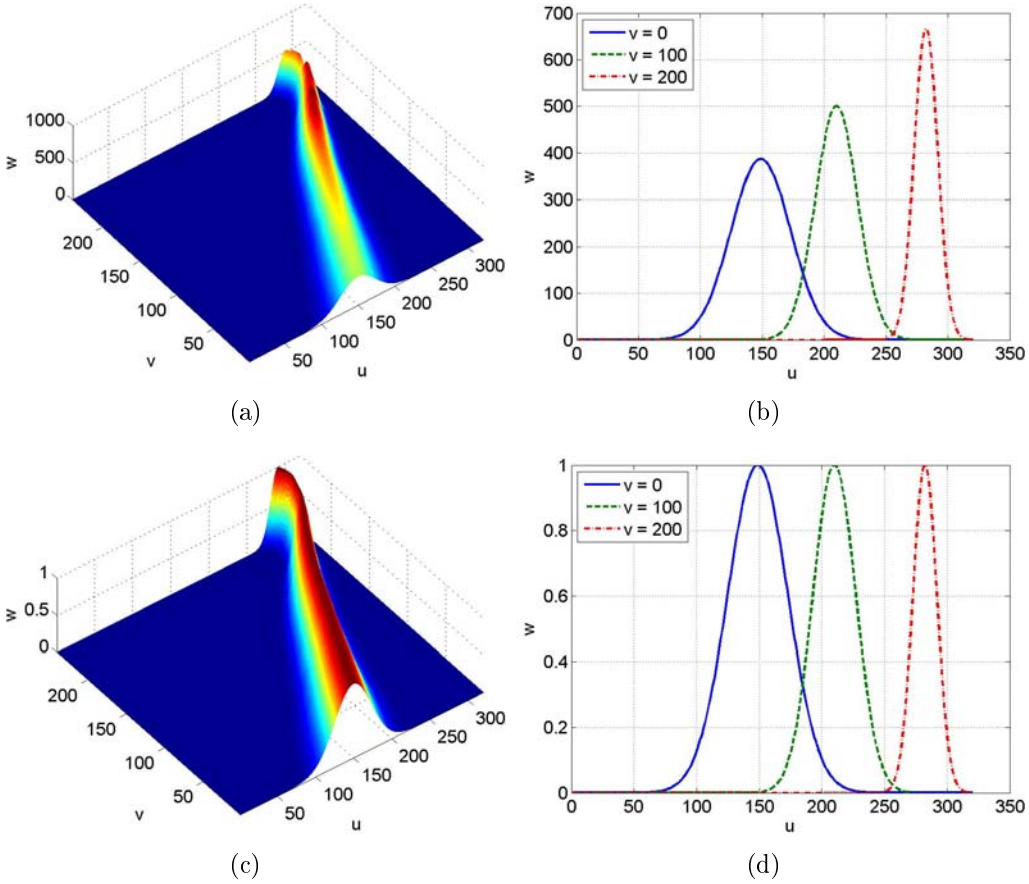

FIGURE 4. Surface curves obtained from histogram fitting process: (a) fitted histogram with smooth surface; (b) fitted Gaussian curves with gradual decrease of standard deviation with respect to the increase of v value; (c) normalized fitted curve provides better visualization of the lane; (d) normalization process preserves the mean and standard deviation of the curves

4.3. **Lane fitting.** From the Gaussian parameters (mean and standard deviation) obtained for every v value, the model fitting process moves on to the subsequent stage: i.e., lane width fitting and center line fitting. In Section 2, the lane width is assumed to be quarter of the standard deviation $\sigma_u(v)$, which is also linearly dependent on the variable v as shown in Equation (5). With a simple least square method, the linear line can be determined with the result constants $k_1 = -0.0738$ and $k_2 = 24.5193$. Figure 5 presents a noisy line and the corresponding best-fit line. The noisy line is plotted with the standard deviation $\sigma_u(v)$ obtained from the histogram fitting process. By comparing the two lines, larger error is expected for greater v value due to a larger non-road region being included in the image plane at the v value. Every pixels from the non-road region can be considered as a noise source in the recorded video.

Most of the existing research work considers a lane to be either linear, parabola or cubic. In this paper, the investigation is extended to degree-8 polynomial. Table 2 shows the coefficients of the fitted polynomials from degree-1 to degree-8 for the center of the lane. The Mean Squre Error (MSE) between the mean $\mu_u(v)$ collected from histogram fitting process and the fitted polynomials are also shown in Table 2. It is observed that the MSE reduces as the degree number increases. Practically, it can be assumed that the MSE reduces in an exponential trend manner, in which the exponential function saturates

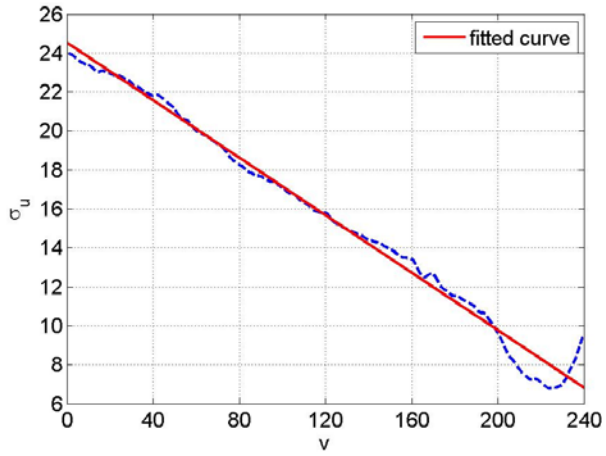

FIGURE 5. Best-fit line for a noisy standard deviation. The noisy line is plotted with the standard deviations obtained from the histogram fitting process.

TABLE 2. Fitted polynomials of different orders for the center of the lane

Order		1	2	3	4	5	6	7	8
MSE		7.7793	6.1186	5.6242	2.2266	2.2255	2.2252	2.2237	2.2194
Coefficient	a_0	302.28	305.20	303.29	297.59	297.59	297.59	297.59	297.59
	a_1	−0.66520	−0.73755	−0.64355	−0.17905	−0.17888	−0.17888	−0.17888	−0.17888
	a_2		3.00E-4	−6.73E-4	−9.30E-3	−9.31E-3	−9.31E-3	−9.31E-3	−9.31E-3
	a_3			2.69E-6	5.83E-5	5.84E-5	5.84E-5	5.84E-5	5.84E-5
	a_4				−1.15E-7	−1.16E-7	−1.16E-7	−1.16E-7	−1.16E-7
	a_5					4.50E-13	4.03E-13	4.03E-13	4.03E-13
	a_6						2.16E-16	−6.39E-16	−6.39E-16
	a_7							3.84E-18	−5.27E-18
	a_8								4.06E-20

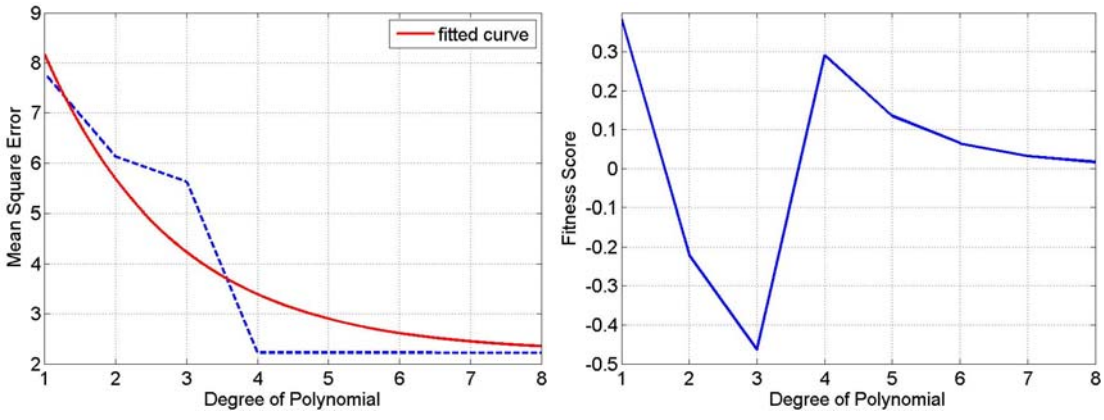

(a) (b)

FIGURE 6. Fitness of polynomials for the center of lane. (a) Mean Square Error (MSE) reduces as the degree of the polynomial increases. The smooth exponential decay function indicates the expected MSE. (b) Fitness score is for different polynomial degrees.

to the MSE of the highest degree polynomial in the study. Figure 6(a) presents the MSE for different polynomial degrees, along with the fitted exponential decay function.

Let $e(n)$ and $\varepsilon(n)$ denote the exponential decay function and MSE of the fitted polynomial respectively. The difference $e(n) - \varepsilon(n)$ can be used as a parameter to measure

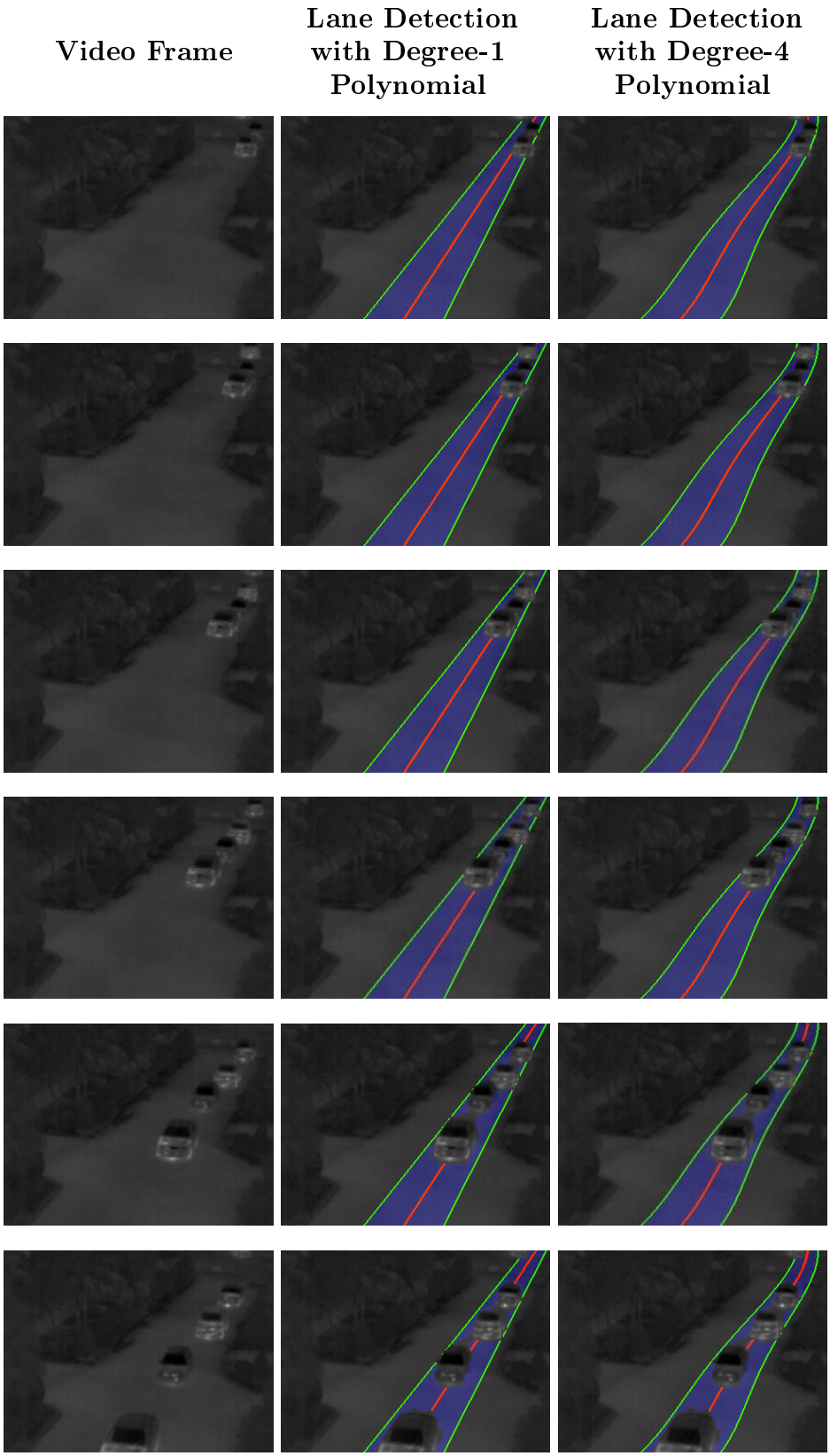

FIGURE 7. Lane detection at the absence of lane markings. The left column presents some example video frames. The middle column presents the detected lane on the frames with degree-1 polynomial. The right column presents the detected lane on the frames with degree-4 polynomial.

the suitability of representing the center line of the lane with the degree-n polynomial. A positive value means that the polynomial represents the center line more accurately than expected. Thus, the positive value indicates that the particular polynomial is suitable and a negative value means the contrary. However, the MSE is generally reduced by increasing the degree (or complexity) of the polynomial. The normalized difference as shown in Equation (6) can be used as a better parameter to measure the fitness. $s(n)$ denotes the fitness score for degree-n polynomial.

$$s(n) = \frac{e(n) - \varepsilon(n)}{n} \tag{6}$$

The fitness score for different polynomial degrees are presented in Figure 6(b). It follows that degree-1 polynomial has the highest score $s(n) = 0.3844$. Thus, the lane can be considered to be linear. Meanwhile, degree-4 polynomial has the second highest score $s(n) = 0.2907$ due to the normal driver behavior to cope with the road condition. There is no lane marking to clearly indicate that there are actually two lanes presence on the road, with one of the lanes being closed. Figure 7 presents the detected lane on the video frames with degree-1 polynomial and degree-4 polynomial. In each frame, the center line indicates the center of the lane and the other two lines indicate the boundary of the lane. The distance between the two boundaries is $4 \times \sigma_u(v)$. The shaded area is the lane region. It can be clearly seen that only one side of the road is detected and considered as the lane without any lane markings on the road.

5. **Conclusions.** Thermal vision provides an alternative for roadway surveillance with good accuracy under various luminance conditions, especially at nighttime. However, the efficiency of most existing marking-based lane detection system deteriorates in poor luminance when lane markings are vague or disappear from the video screen. In this paper, a Gaussian-based road model is proposed as an alternative technique, where the lane is detected based on least square method. The detected lane is considered to be the best-fit lane on the image plane. A video is recorded using a thermal camera at the traffic scene and the road with the absence of lane markings has been chosen. In this investigation, the proposed method is able to detect the lane and also the width of the lane without any lane marking. In addition, the method is also capable of determining whether the lane is linear or polynomial to certain degree.

REFERENCES

[1] N. Paragois and R. Deriche, Geodesic active contours and level sets for the detection and tracking of moving objects, *IEEE Trans. Pattern Analysis and Machine Intelligence*, vol.22, no.3, pp.266-280, 2000.

[2] Z. Kim and J. Malik, Fast vehicle detection with probabilistic feature grouping and its application to vehicle tracking, *IEEE International Conference on Computer Vision*, Nice, France, 2003.

[3] X. Ji, Z. Wei and Y. Feng, Effective vehicle detection technique for traffic surveillance systems, *Journal of Visual Communication & Image Representation*, pp.647-658, 2006.

[4] Y. Li, Z. Li, H. Tian and Y. Wang, Vehicle detecting and shadow removing based on edged mixture Gaussian model, *Proc. of the 18th IFAC World Congress*, Milano, Italy, 2011.

[5] R. Taktak, M. Dufaut and R. Husson, Vehicle detection at night using image processing and pattern recognition, *IEEE International Conference on Image Processing*, 1994.

[6] R. Cucchiara, M. Piccardi and P. Mello, Image analysis and rule-based for a traffic monitoring system, *IEEE Trans. Intelligent Transportation Systems*, vol.1, no.2, pp.119-130, 2000.

[7] Y. Yue, A traffic-flow parameters evaluation approach based on urban road video, *International Journal of Intelligent Engineering & Systems*, vol.2, no.1, pp.33-39, 2009.

[8] W. Zhang, Q. M. J. Wu and G. Wang, Vehicle headlights detection using Markov random fields, *Asian Conference on Computer Vision*, Xi'an, China, 2009.

[9] Q. Zou, H. Ling, S. Luo, Y. Huang and M. Tian, Robust nighttime vehicle detection by tracking and grouping headlights, *IEEE Trans. Intelligent Transportation Systems*, vol.16, no.5, pp.2838-2849, 2015.

[10] Z. Wang and B. G. Cai, A ROI setting method for vehicle detection in urban environment, *IEEE-APS Topical Conference on Antennas and Propagation in Wireless Communications*, Cape Town, 2012.

[11] K. Huh, J. Park, J. Hwang and D. Hong, A stereo vision-based obstacle detection system in vehicles, *Optics and Lasers in Engineering*, vol.46, no.2, pp.168-178, 2008.

[12] N. Arshad, K.-S. Moon, S.-S. Park and J.-N. Kim, Lane detection with moving vehicles using color information, *Proc. of the World Congress on Engineering and Computer Science*, San Francisco, 2011.

[13] A. M. Muad, A. Hussain, S. A. Samad, M. M. Mustaffa and B. Y. Majlis, Implementation of inverse perspective mapping algorithm for the development of an automatic lane tracking system, *IEEE Region 10 Conference*, 2004.

[14] X. Liu, B. Dai, J. Song, H. He and B. Zhang, Real-time long-range lane detection and tracking for intelligent vehicle, *International Conference on Image and Graphics*, Hefei, China, 2011.

[15] T. Kasai and K. Onoguchi, Lane detection system for vehicle platooning using multi-information map, *International IEEE Conference on Intelligent Transportation Systems*, Funchal, 2010.

[16] J. Liu and M. Wang, An approach for lane segmentation in traffic monitoring systems, *International Conference on Multimedia Information Networking and Security*, 2009.

[17] C. F. Wu, C. J. Lin, H. Y. Lin and H. Chung, Adjacent lane detection and lateral vehicle distance measurement using vision-based neuro-fuzzy approaches, *Journal of Applied Research and Technology*, vol.11, no.2, pp.251-258, 2013.

[18] N. B. Romdhane, M. Hammami and B.-A. Ben-Abdallah, A lane detection and tracking method for driver assistance system, *Knowledge-Based and Intelligent Information and Engineering Systems*, pp.407-417, 2011.

[19] J. He, H. Rong, J. Gong and W. Huang, A lane detection method for lane departure warning system, *International Conference on Optoelectronics and Image Processing*, Haikou, China, 2010.

[20] J. Wang, F. Gu, C. Zhang and G. Zhang, Lane boundary detection based on parabola model, *IEEE International Conference on Information and Automation*, Harbin, China, 2010.

[21] M. Haloi and D. B. Jayagopi, A robust lane detection and departure warning system, *IEEE Intelligent Vehicles Symposium*, Seoul, Korea, 2015.

[22] Q.-B. Truong and B.-R. Lee, New lane detection algorithm for autonomous vehicles using computer vision, *International Conference on Control, Automation and Systems*, Seoul, Korea, 2008.

[23] H. Tan, Y. Zhou, Y. Zhu, D. Yao and K. Li, A novel curve lane detection based on improved river flow and RANSA, *IEEE International Conference on Intelligent Transportation Systems (ITSC)*, Qingdao, China, 2014.

[24] P. G. Ducksbury, D. M. Booth and C. J. Redford, Vehicle detection in infrared linescan imagery using belief networks, *International Conference on Image Processing and Its Applications*, 1995.

[25] L. Andreone, P. C. Antonello, M. Bertozzi, A. Broggi, A. Fascioli and D. Ranzato, Vehicle detection and localization in infra-red images, *IEEE International Conference on Intelligent Transportation Systems*, Singapore, 2002.

[26] A. Sangnoree and K. Chamnongthai, Robust method for analyzing the various speeds of multitudinous vehicles in nighttime traffic based on thermal images, *International Conference on Computer Sciences and Convergence Information Technology*, 2009.

[27] S. Der, A. Chan, N. Nasrabadi and H. Kwon, Automated vehicle detection in forward-looking infrared imagery, *Applied Optics*, vol.43, no.2, pp.333-348, 2004.

[28] Y. Iwasaki, A method of robust moving vehicle detection for bad weather using an infrared thermography camera, *International Conference on Wavelet Analysis and Pattern Recognition*, Hong Kong, 2008.

[29] Y. Iwasaki, M. Misumi and T. Nakamiya, Robust vehicle detection under various environmental conditions using an infrared thermal camera and its application to road traffic flow monitoring, *Sensors*, vol.13, no.6, pp.7756-7773, 2013.

[30] M. Miman, O. O. Akırmak and H. C. Korkmaz, Lane departure system design using with IR camera for night-time road conditions, *Tem Journal*, vol.4, no.1, pp.54-59, 2015.

[31] M. Aly, Real time detection of lane markers in urban streets, *IEEE Intelligent Vehicles Symposium*, Eindhoven, 2008.

[32] H. Yoo, U. Yang and K. Sohn, Gradient-enhancing conversion for illumination-robust lane detection, *IEEE Trans. Intelligent Transportation Systems*, vol.14, no.3, pp.1083-1094, 2013.
[33] M. Piccardi, Background subtraction techniques: A review, *IEEE International Conference on Systems, Man and Cybernetics*, 2004.
[34] D. Koller, J. Weber, T. Huang, J. Malik and G. Ogasawara, Towards robust automatic traffic scene analysis in real-time, *International Conference on Computer Vision & Image Processing*, 1994.
[35] C. Stauffer and E. Grimson, Adaptive background mixture models for realtime tracking, *IEEE Computer Society Conference on Computer Vision and Pattern Recognition*, 1999.
[36] N. M. Oliver, B. Rosario and A. P. Pentland, A Bayesian computer vision system for modeling human interactions, *IEEE Trans. Pattern Analysis and Machine Intelligence*, vol.22, no.8, pp.831-843, 2002.
[37] T. Bouwmans, Traditional and recent approaches in background modeling for foreground detection: An overview, *Computer Science Review*, vol.11, pp.31-66, 2014.
[38] J. Wang, T. Mei, B. Kong and H. Wei, An approach of lane detection based on inverse perspective mapping, *IEEE International Conference on Transportation Systems*, Qingdao, China, 2014.
[39] B. C. Yeo, W. S. Lim, H. S. Lim and W. K. Wong, Extended fuzzy background modeling for moving vehicle detection using infrared vision, *ICICE Electronics Express*, vol.8, no.6, pp.340-345, 2011.
[40] B. C. Yeo, W. S. Lim and H. S. Lim, Scalable-width temporal edge detection for recursive background recovery in adaptive background modeling, *Applied Soft Computing*, vol.13, no.4, pp.1583-1591, 2013.
[41] Y. Sakamoto, H. Arie, T. Ebinuma, K. Fujii and S. Sugano, Initial value analysis of a nonlinear least-square method for indoor doppler positioning with a single pseudolite, *IEEE Proc. of SICE Annual Conference*, Tokyo, Japan, 2011.
[42] D. C. Montgomery, E. A. Peck and G. G. Vining, *Introduction to Linear Regression Analysis*, 5th Edition, John Wiley & Sons, Hoboken, 2015.
[43] M. A. H. Khan, T. Muntasir, A. S. M. Z. Rahman, U. K. Acharjee and M. A. Layek, Multiple polynomial regression for modeling a MOSFET in saturation to validate the early voltage, *IEEE Symposium on Industrial Electronics and Applications*, Langkawi, Malaysia, 2011.